

EFFECTS OF SIMPLIFIED CHEMICAL KINETIC MODEL ON THE MICRO-FLAME STRUCTURE AND TEMPERATURE OF THE LEAN PREMIXED METHANE-AIR MIXTURES

Junjie Chen^{*}, Xuhui Gao

Henan Polytechnic University, School of Mechanical and Power Engineering, 454000, Jiaozuo, China

*Corresponding author: comcji@163.com

Received: April, 06, 2015

Accepted: June, 24, 2015

Abstract: The effect of simplified chemical kinetic model on the micro-flame structure, central axis and wall temperatures were investigated with different one-step global chemical kinetic mechanisms following Mantel, Duterque and Fernández-Tarrazo models. Numerical investigations of the premixed methane-air flame in the micro-channel and lean conditions were carried out to compare and analyze the effect of the comprehensive chemical kinetic mechanisms. The results indicate that one-step global chemical kinetic mechanism affects both the micro-flame shape and the combustion temperature. Among three simulation models, Mantel model allows a stable micro-flame with a bamboo shoot form, which anchor at the inlet. Duterque model gives a stable elongated micro-flame with a considerable ignition delay, and a dead zone with fluid accumulation is observed at the entrance, which may explain the very high combustion temperature and the fast reaction rate obtained, despite the micro-flame development presents a very hot spot and causes a broadening of the combustion zone. Fernández-Tarrazo model results in a rapid extinction and doesn't seem to take all the kinetic behavior into account for the appropriate micro-combustion simulations.

Keywords: *flame structure, flame temperature, micro-combustion, micro-flame, simplified chemical kinetic model*

INTRODUCTION

Recently, developments of micro power system enable us to minimize the combustors size. Micro-combustion is the sequence of exothermic chemical reaction between fuel and oxidant accompanied by the conversion of chemical species and production of heat at micro level, which characteristic length is shorter than the quenching distance of flame [1]. The micro-combustion characteristics depend on various chemical and physical processes, such as homogeneous and heterogeneous reactions, thermal and mass diffusion, molecular transport, convection and radiation [2].

In practice, there are many severe challenges to maintain stable combustion at micro-scales. The first issue is the wall radical capture and increased heat losses as a result of increase of surface-to-volume ratio, which always causes flame quenching on the wall [3, 4]. Another critical issue is the limited residence time of the fuel-oxidant mixtures in micro-combustors [5]. Due to the adversity under decreasing scale, micro-flame exhibits many unusual behaviors [6]. For example, flames with repetitive ignition and extinction were experimentally observed [7, 8]. Deshpande and Kumar [9] and Xu and Ju [10] observed X-shaped spinning flames in stepped and divergent micro-tubes. Experimental investigation on miniature-scale liquid-fuel-film combustor by Sirignano *et al.* [11] demonstrated internally and externally anchored flame modes. Spiral flame and Pelton-wheel-like flame were reported by Fan *et al.* [12] and Kumar *et al.* [13].

The tools of numerical simulation have permitted to solve the issues of propagation of self-sustained flame in micro-combustors [14, 15]. In order to get an in-depth understanding on the structure of micro-flames, flame stability along with the interactions between wall and flame have been investigated [16, 17]. The use of numerical simulation to investigate the micro-combustion characteristics requires judicious choices of the chemical kinetic mechanisms.

Many efforts to generate chemical kinetic models with simple chemistry mechanisms can be trace back to the previous works of Westbrook and Dryer [18], who proposed several simplified reaction mechanisms (one and two global reaction steps as well as quasi-global mechanisms) models for different hydrocarbon fuels. Their developments were based on the computations of premixed laminar flames, leading to a series of the optimum chemical kinetic parameters (pre-exponential factor, activation energy and reaction orders) that best fitted the main reaction rate parameters of premixed combustion. The aforementioned models were also successfully verified in the micro-combustion investigations with reliable results during the last decade. For example, D.G. Vlachos *et al.* [19, 20] used a one-step chemical kinetic mechanism to investigate; optimal reactor dimensions for the homogeneous combustion in micro-channels [19], extending the region of stable homogeneous combustion through forced unsteady operation at micro-scales [20], and the flame stability and combustion characteristics at micro-scales [19, 20]. Recently, Gutkowski [21] used a single-step global reaction mechanism to perform the numerical investigation of ignition methods effect on micro-flame behavior during passing through the sudden contraction and isothermal cold walls near the quenching conditions in small channels. However, in all aforementioned works, it was obliged to adjust the fuel exponent value to avoid the simulation failure.

Some simplified models with single-step overall equation were also proposed in addition to Westbrook and Dryer's mechanisms. Fernández-Tarrazo *et al.* [22] tested a simple one-step Arrhenius model for partially premixed hydrocarbon combustion.

Mantel *et al.* [23] used a stoichiometric concentration exponent's model and proposed a new methodology to determine the kinetic parameters for one- and two-step chemical models. The Duterque model [24] was used to investigate comparison of different chemical kinetic mechanisms of methane combustion [25].

The Fernández-Tarrazo, Mantel and Duterque models are adapted the Arrhenius models, and have been testified to accurately describe the macro-combustion phenomenon of hydrocarbons. However, these models have not yet been studied in micro-combustors. Therefore, it is extremely interesting to analyze the stability, production and overall micro-flame behavior with the aforementioned three models, through the numerical simulations in micro-combustors. The main purpose of this paper is to explore the effect of different chemical kinetic mechanisms on the flame shape and position in micro-combustors. These three different chemical kinetic models are used to perform the numerical simulation of the premixed methane-air micro-combustion. Several parameters are investigated, for instance, reaction rate, axial temperature of reacting flow, wall temperature, position and shape of micro-flame in fuel-lean conditions.

NUMERICAL MODELS AND SIMULATION APPROACH

Model geometry

A schematic view of the parallel plates is shown in Figure 1. The FLUENT [26] coupled with the CHEMKIN [27] was used to simulate the fluid flow in the micro-channel of height $H = 0.8$ mm, length $L = 4.0$ mm, and solid wall thickness $\delta = 0.2$ mm. The solid wall material of plane channel is alumina. The original point is fixed at the inlet center, x represents the downstream or axial distance, while y depicts the vertical distance or the distance from centerline of the micro-channel.

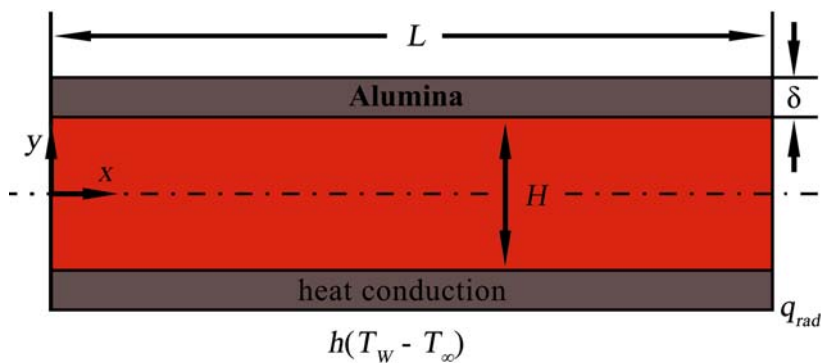


Figure 1. Schematic diagram of the micro-channel geometry

Mathematical model

In order to couple the homogeneous reaction, heat transfer, transport and concentrated species, and fluid dynamics modules, an external program CHEMKIN is used as user defined function to FLUENT to extend the modeling capabilities in simulating the

detailed chemical kinetics. The governing equations for steady, laminar, reactive gas flow with homogeneous reactions are as follows:

Continuity equation:

$$\frac{\partial \rho}{\partial t} + \nabla \cdot (\rho \underline{u}) = 0 \quad (1)$$

Momentum equation:

$$\rho \left(\frac{\partial \underline{u}}{\partial t} + \underline{u} \cdot \nabla \underline{u} \right) = -\nabla p_l + \nabla \cdot (\mu \underline{\underline{S}}) \quad (2)$$

$$\underline{\underline{S}} = \nabla \underline{u} + (\nabla \underline{u})^T - \frac{2}{3} (\nabla \cdot \underline{u}) \underline{\underline{I}} \quad (3)$$

Energy equation:

$$\rho C_p \left(\frac{\partial T}{\partial t} + \underline{u} \cdot \nabla T \right) = \nabla \cdot (\lambda \nabla T) - \sum_{i=1}^{N_g} h_i \dot{\omega}_i - \rho \left(\sum_{i=1}^{N_g} C_{p,i} Y_i \underline{V}_i \right) \cdot \nabla T \quad (4)$$

$$C_p = \sum_{i=1}^{N_g} C_{p,i} Y_i \quad (5)$$

Composition equation:

$$\rho \left(\frac{\partial Y_i}{\partial t} + \underline{u} \cdot \nabla Y_i \right) = -\nabla \cdot (\rho Y_i \underline{V}_i) + \dot{\omega}_i \quad i = 1, \dots, N_g \quad (6)$$

State equation:

$$p_0 = \frac{\rho R T}{\bar{W}} \quad (7)$$

$$\bar{W} = \left(\sum_{i=1}^{N_g} \frac{Y_i}{W_i} \right)^{-1} \quad (8)$$

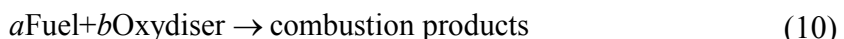
Since heat transfer along the wall significantly affects the flame stability [20], heat transfer along the solid wall is considered in this model. The appropriate energy equation for the solid phase is given as follow:

$$\frac{\partial (k_s \partial T)}{\partial x^2} + \frac{\partial (k_s \partial T)}{\partial y^2} = 0 \quad (9)$$

where k_s ($\text{W} \cdot \text{m}^{-1} \cdot \text{K}^{-1}$) denotes the thermal conductivity of solid wall.

Chemical kinetics

In the present work, five species (hydrocarbon, oxygen, water, nitrogen and carbon dioxide) and one simplified chemical kinetic equation were chosen.



The source term is calculated by reaction rate equation:

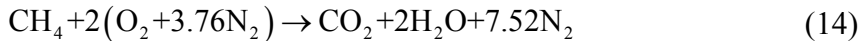
$$R_j = k^f \prod_{i=1}^{Q_f} c_j^v \quad (11)$$

$$k^f = A T^n \exp \left(-\frac{E_a}{R_g T} \right) \quad (12)$$

The reaction rate equation is given as follows:

$$R_j = AT^n \exp\left(-\frac{E_a}{R_g T}\right) c_{\text{Fuel}}^a c_{\text{Oxydant}}^b \quad (13)$$

Chemical equation:



In the equations (11), (12) and (13) R_j ($\text{mol}\cdot\text{m}^{-3}\cdot\text{s}^{-1}$) are the reaction rate of species j ; v is the partial reaction order with respect to species j ; k^f ($\text{1}\cdot\text{s}^{-1}$) is the reaction rate constant; Q_j is the species quantity; A is the pre-exponential factor; R_g ($8.314 \text{ J}\cdot\text{mol}^{-1}\cdot\text{K}^{-1}$) is the molar gas constant; T (K) is the temperature; n is the temperature exponent; E_a ($\text{J}\cdot\text{mol}^{-1}$) is the activation energy; c ($\text{mol}\cdot\text{m}^{-3}$) is the concentration; a and b are the partial reaction orders or the concentration exponents.

In the equation (13), the unknown parameters is the activation energy E_a , concentration exponents a and b , pre-exponential factor A , which are defined through the comparative simulation between the flow velocity, the flame speed and the experimental data [28]. Each aforementioned parameter has to be determined. When simulating combustion phenomena by FLUENT coupled with the CHEMKIN, chemical kinetic mechanism is the equation (15) below, nevertheless, Westbrook and Dryer [18], found that to stabilize the micro-flame, the concentration exponents cannot be those defined as presented in equation (15) from the stoichiometric conditions, rather they must comply with the following conditions, which require to find them.

$$R = AT^n \exp\left(-\frac{E_a}{R_g T}\right) c_{\text{Fuel}}^1 c_{\text{Oxydant}}^2 \quad (15)$$

$$0 < a \ll 1 \text{ and } 0 < b \ll 2 \quad (16)$$

The determination of parameters (concentration exponent, activation energy, and pre-exponential factor) demands more numerical simulations that depend on several factors, for instance, the transport properties of fluid, the composition of mixture and even the mesh size [21]. Comprehensive overview of numerical simulations with simplified and detailed chemical kinetic mechanisms in micro-channels is shown in Table 1.

The choice of selected models for this study is dictated by their wide usage and simplicity. These are defined by the following equations (17-19).

$$R_{\text{CH}_4} \left(\text{mol}/\text{m}^3 \cdot \text{s} \right) = 9.1 \times 10^{19} \exp\left(-\frac{1.045 \times 10^5}{R \cdot T}\right) c_{\text{CH}_4}^1 \cdot c_{\text{O}_2}^2 \quad (17)$$

$$R_{\text{CH}_4} \left(\text{mol}/\text{m}^3 \cdot \text{s} \right) = 6.9 \times 10^8 \exp\left(-\frac{1.321 \times 10^5}{R \cdot T}\right) c_{\text{CH}_4}^1 \cdot c_{\text{O}_2} \quad (18)$$

$$R_{\text{CH}_4} \left(\text{mol}/\text{m}^3 \cdot \text{s} \right) = 1.5 \times 10^{13} \exp\left(-\frac{2.03 \times 10^5}{R \cdot T}\right) c_{\text{CH}_4}^{0.7} \cdot c_{\text{O}_2}^{1.3} \quad (19)$$

The reaction rates and thermodynamic properties were evaluated using FLUENT coupled with the CHEMKIN [27, 36, 37], while the transport properties were computed using CHEMKIN's transport library [38].

Table 1. Comprehensive overview of numerical simulations with simplified and detailed chemical kinetic mechanisms in micro-channels

Fuel-oxidizer	Combustor geometry	Combustor size	Reaction mechanism	Ref.
CH ₄ /air fuel-lean	Plane channel	H = 1.0 mm L = 10.0 mm	Detailed gas-phase and surface reactions	[29]
C ₃ H ₈ /air	Parallel plates	H = 0.6 mm L = 10.0 mm	One-step global reaction	[30]
CH ₄ /air ($\varphi = 0.9$)	Parallel plates	H = 0.6 mm L = 10.0 mm	One-step global reaction	[20]
H ₂ /air ($\varphi = 0.9$)	Cylindrical chamber	d = 0.1 mm	Detailed gas-phase reactions	[31]
CH ₄ /air, C ₃ H ₈ /air ($\varphi = 0.9$)	Parallel plates	H = 0.6 mm L = 10.0 mm	One-step global reaction	[19]
H ₂ /air ($\varphi = 0.5$)	Cylindrical tube and parallel plates	d = 0.4-0.8 mm	Detailed gas-phase reactions	[32]
CH ₄ /air ($\varphi = 0.9$)	Cylindrical tube and parallel plates	d = 1.0-2.0 mm	Detailed gas-phase reactions	[33]
CH ₄ /air	Cylindrical tube	d = 2.0 mm	One-step global reaction	[34]
H ₂ /air	Parallel disk	H = 0.15-0.3 mm	One-step global reaction	[35]
CH ₄ /air ($\varphi = 0.9$)	Cylindrical tube with sudden contraction	d = 1.6-6.0 mm	One-step global reaction	[21]

In the present work, the sensitivity analysis of the micro-flame stability of premixed methane-air mixtures will be carried out through three chemical kinetics models (Fernández-Tarrazo, Mantel and Duterque models) with one-step global equation, respectively defined by equations (17-19). The obtained results from numerical simulations will be compared with those existing in the literatures taking as reference cases, Li *et al.* [33] who used detailed chemical kinetic mechanisms, Norton and Vlachos [20] who used an overall one-step global reaction kinetic mechanism.

Boundary conditions

The boundary conditions used in this model are as follows. Uniform profiles for the species concentrations, the temperature, and the axial velocity are specified at the inlet. The incoming methane-air flow ($\varphi = 0.9$) was fully premixed with the inlet velocity of 0.5 m·s⁻¹, and had uniform inlet temperature of 300 K. At the exit, the pressure was specified and the remaining variables were calculated assuming far-field conditions, namely, zero diffusive flux of species or energy normal to the exit. A symmetry boundary condition was employed at the centerline between the two parallel plates. No-slip boundary condition was imposed at fluid-wall interface; the heat flux at this gas-wall interface was calculated using Fourier's law along with continuity in temperature and heat flux was ensured. For the energy and species equations, Danckwerts boundary conditions were employed. The 2D energy equation was solved in the bulk of the wall. Moreover, the thermal boundary condition at the solid wall of the micro-combustors is the heat loss to the ambient air. The radiation between the inner surfaces of the wall was considered using the discrete ordinates model. The external surface of the wall, heat

losses to the surroundings were calculated through equation (20), in which both natural convection and thermal radiation were considered.

$$q = h(T_{w,o} - T_{ref}) + \varepsilon\sigma(T_{w,o}^4 - T_{ref}^4) \quad (20)$$

where q is the heat flux; h is the external heat transfer coefficient; $T_{w,o}$ is the temperature at the external surface; ε is the emissivity of the solid surface and σ is the Stephan-Boltzmann constant ($5.67 \times 10^{-8} \text{ W}\cdot\text{m}^{-2}\cdot\text{K}^{-4}$).

Computation scheme

In the present work, the uniform grid size of $0.5 \mu\text{m}$ was used to mesh the numerical models for all scenarios analyzed. Grid independence were examined. The aforementioned conservation equations were solved implicitly with the 2D steady-state double-precision segregated solver using the under-relaxation method. The momentum, species, and energy equations were discretized using second-order upwind scheme. The “SIMPLE” algorithm was used to couple the pressure and velocity. The fluid density was calculated using the ideal gas law. The fluid thermal conductivity, specific heat, and viscosity were calculated using the mass fraction weighted average of species properties. The species specific heat was calculated using the piecewise polynomial fit of temperature. The convergence of CFD simulation was judged based on the residuals of all governing equations. The simulation results were achieved with residuals smaller than 1.0×10^{-6} . The simulations were performed on a high-performance cluster consisting of $4 \times \text{E5-2600}$ processors and 48 GB of RAM. Parallel processing was used, and the message passing interface (MPI) was used to transmit information between nodes. In order to achieve convergence as well as compute extinction points, natural parameter continuation was implemented. The calculation time of each simulation varied between 6.0 and 20.0 hours, depending on the difficulty of the problem, the initial guess, and chemical kinetic mechanisms.

RESULTS AND DISCUSSION

In the present work, the effects of one-step global chemical kinetic mechanism on the micro-flame structure, central axis and wall temperatures are investigated numerically to explore the effect of different mechanisms (Fernández-Tarrazo, Mantel and Duterque models) on flame characteristics at the micro-scale.

Reference cases

In this section, two works (detailed and simplified kinetic mechanisms) on the micro-flame of the premixed methane-air mixtures for the comprehensive kinetic model equation are chosen as a framework to assess and compare with the relevance of our simulations results.

Li *et al.* [33] performed numerical studies on micro-flame of premixed methane-air mixtures through a micro-reactor (cylindrical tube and 2D parallel plates, $H = 1.0 \text{ mm}$), and detailed chemical kinetics mechanisms were employed with 16 species and 25 reversible reactions. The mechanisms can better represent the reaction process as

they involve partial oxidation, reverse reactions and intermediate products. In addition, the following assumptions are made: no Dufour effects; no gas radiation; no work done by pressure and viscous forces; and steady-state. They found that a convex steady micro-flame, the initial preheating temperature T_i is 1600 K, the initial velocity V_i is $0.5 \text{ m}\cdot\text{s}^{-1}$, and the initial temperature T_i is 300 K. From the temperature profile analysis, we found that, with the same initial temperature T_i before preheating, the fluid passes the axial distance of 2.8 mm then reaches the ignition temperature of 1200 K. The temperature of fluid increases to reach the maximum of 1850 K at the axial distance of 2.8 mm then decreases slightly to 1800 K. From this study, it can be underlined that the detailed chemical kinetics mechanisms provide the temperature below the adiabatic flame temperature of methane.

Norton and Vlachos [20] investigated theoretically and numerically the flame stability and combustion characteristics of premixed methane-air mixtures at the micro-scale. The primary focus of their work is on understanding the effect of wall heat transfer within the micro-combustor. They proposed the numerical investigation by using a reduced methane combustion mechanism (one-step irreversible reaction kinetic model) provided by Westbrook and Dryer [18]. The initial temperature of preheating the incoming fluid for all simulations was 1273 K to allow the fluid ignition. A stable flame with inlet velocity of $0.3 - 0.8 \text{ m}\cdot\text{s}^{-1}$, and in fuel-lean conditions ($\varphi = 0.9$) was simulated. The predicted temperature of micro-flame reached a maximum of 2270 K at the distance $x = 1.8 \text{ mm}$ from the inlet of the micro-combustor, although the maximum temperature reached is overestimated because of exceeding the adiabatic flame temperature. The exit temperature of the micro-combustion products was evaluated as 1480 K, while the wall temperature ranged from 1273 K at the inlet, and reached the peak of 1560 K at the combustion zone, then after a slight decline in temperature up to 1480 K at the exit. From this study, it appears that the global kinetic model allows numerical simulation of the micro-flame and can lead to the reliable analysis of micro-combustor parameters.

Effect on the micro-flame structure

Three chemical kinetics models (Mantel, Duterque and Fernández-Tarrazo models with one-step global equation) simulated the stable micro-flame were observed, however, their flame shapes are completely different from each other.

The micro-flame obtained with Mantel model is shown in Figure 2(a), the stable micro-flame developed with a particularly bamboo shoot shape at the inlet is observed. Hackert *et al.* [39] investigated the flame shape and propagation speed in parallel plates and cylindrical ducts, and observed the flame is the tulip-shaped in the micro-channel, however, the same convex micro-flame is found in the previous works of Li *et al.* [33]. The developed thickness of the micro-flame can be estimated at 1.6 mm, which is about an order of magnitude of the thickness value of the micro-flame produced with gaseous fuel. The mass fraction of methane is shown in Figure 2(b), it is clear that entire methane is consumed in the combustion zone, the mass fraction of methane is 0.055 at the inlet, and only after 2.0 mm it becomes zero as observed.

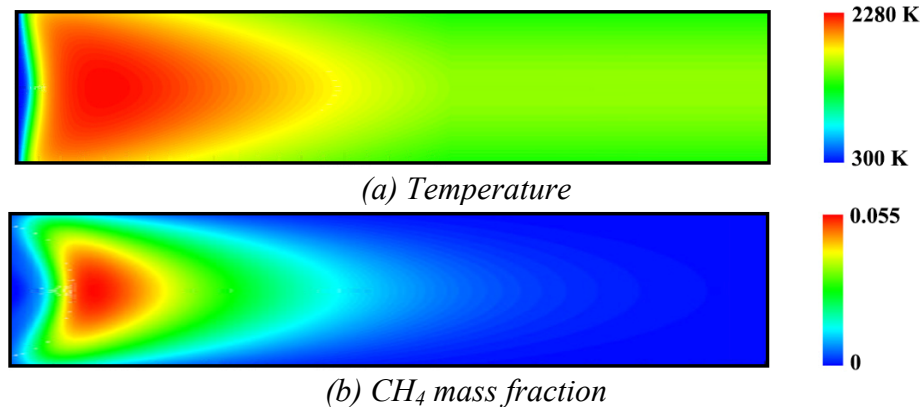


Figure 2. Contours of temperature and CH_4 mass fraction, resulting of Mantel model

The fact, the concentration exponents meet the stoichiometric coefficients of the methane combustion, can explain the entire methane oxidation.

Figure 3(a) shows that the temperature of fluid increases to reach the maximum of 2280 K at the axial distance of 0.4 mm then decreases slightly to 1480 K. The profile of CH_4 reaction rate is shown in Figure 3(b), which appears that the CH_4 combustion is very rapid despite the small micro-flame thickness; the gas-phase combustion is limited and complete in the flow space.

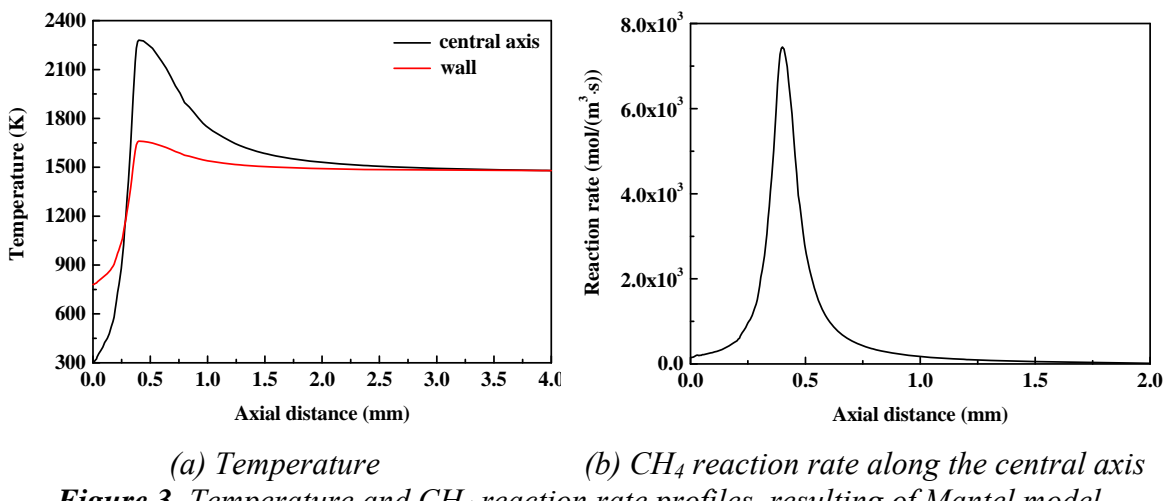


Figure 3. Temperature and CH_4 reaction rate profiles, resulting of Mantel model

The predicted micro-flame with Duterque model is shown in Figure 4(a). In this case, the micro-flame begins to take shape after 0.8 mm, and therefore it much later than that simulated numerically with the Mantel model. As observed, the micro-flame obtained is tulip-shaped, and the combustion zone is broadened, which increase a blowout risk with the thickness greater than 2.2 mm. This broadening of the combustion zone can be explained by the fluid accumulation that seems to exist at the inlet, and the reason is that the ignition process is not instantaneous. The mass fraction of methane is shown in Figure 4(b). It appears that complete conversion is achieved after 2.8 mm.

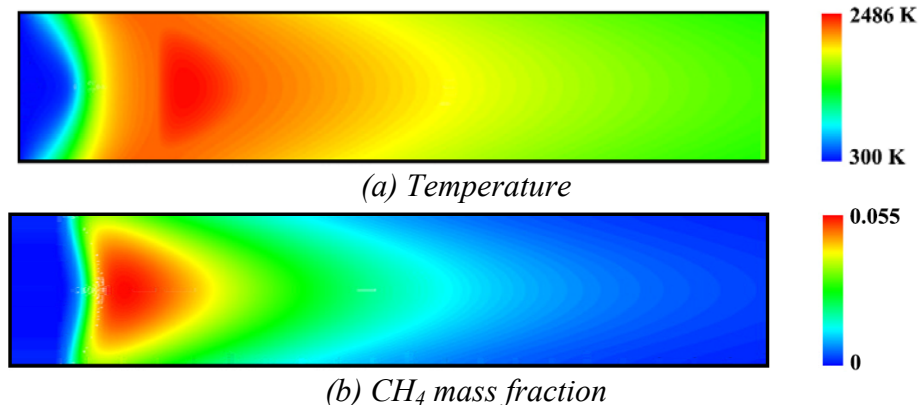


Figure 4. Contours of temperature and CH_4 mass fraction, resulting of Duterque model

Figure 5(a) shows that the temperature of fluid increases to reach the maximum of 2486 K at the axial distance of 0.8 mm. Therefore, the hot spot in this space can cause the material to melt and damage the wall. The methane-air mixtures burn so much longer, which may be confirmed by the CH_4 reaction rate profile in Figure 5(b).

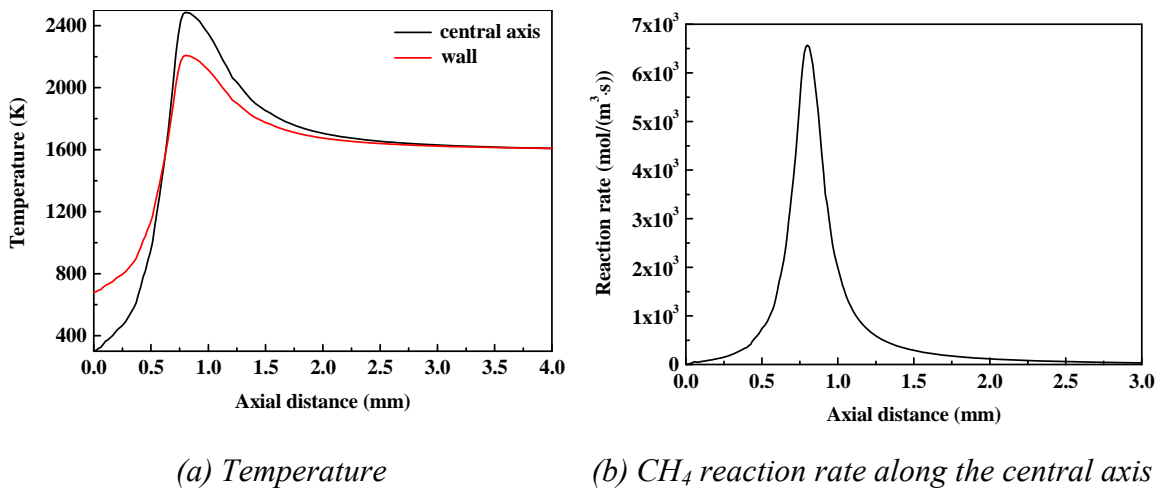


Figure 5. Temperature and CH_4 reaction rate profiles, resulting of Duterque model

The predicted micro-flame with Fernández-Tarrazo model is shown in Figure 6(a). In this case, the reaction rate of methane oxidation is very fast, and the combustion process occurs quite at the inlet with instantaneous quench. The flashback risk is high, because the gas phase reaction zone is relatively narrow. The micro-flame obtained has the cone-shape, and the high temperature zone mainly located near the inlet. The mass fraction of methane is shown in Figure 6(b), which shows that the conversion of methane is partial and highly incomplete.

Figure 7(a) shows that the temperature of fluid increases to reach the maximum of 1606 K at the axial distance of 0.06 mm then decreases quickly to 1107 K at $x = 0.8$ mm. The CH_4 reaction rate profile as observed in Figure 7(b) confirmed that the methane oxidation proceeds on a thin layer. The previous works of Westbrook and Dryer [18] predicted that the methane combustion with such model is impossible.

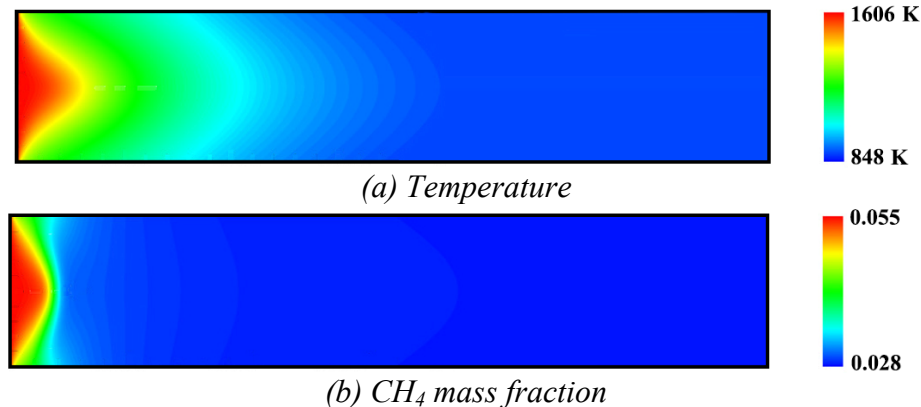


Figure 6. Contours of temperature and CH_4 mass fraction, resulting of Fernández-Tarrazo model

However, many years later, Fernández-Tarrazo *et al.* [22] demonstrated that, in the case of macro combustion, such model with lean combustion could be applied, which does not seem to be suitable for use the micro-combustion case, at least for the configuration of the parallel plate simulated in this work.

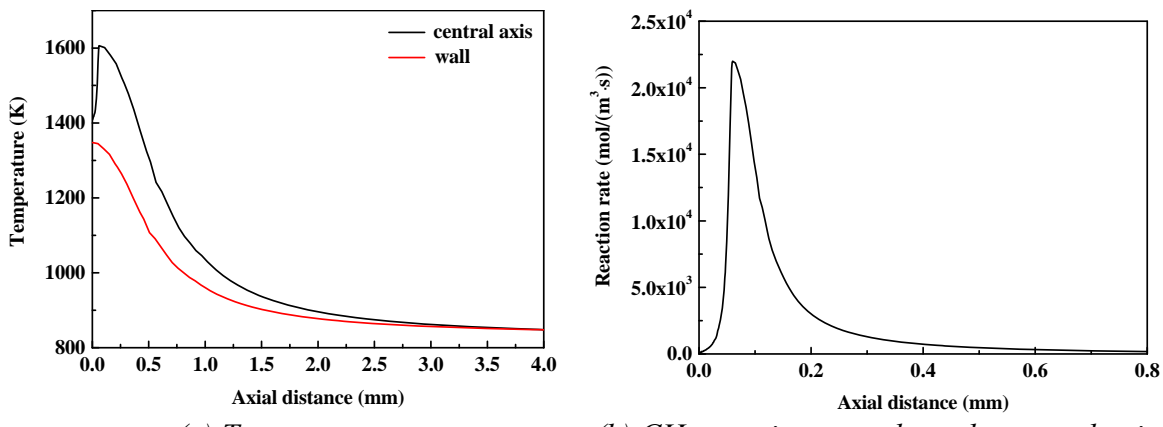


Figure 7. Temperature and CH_4 reaction rate profiles, resulting of Fernández-Tarrazo model

The simulation results clearly show that the one-step global chemical kinetic model has a significant effect on the combustion process of the overall flame structure in micro-combustors.

Effect on the central axis temperature

The temperature profile obtained with the Mantel model is shown in Figure 3(a), the initial inlet temperature of premixed methane-air mixtures is 300 K, and the temperature begins to increase after 0.05 mm. The temperature jump to 900 K, contacting with the wall preheats the reactants. Once the temperature of the reactants reaches approximately 950 K, the ignition switches on the reaction mixtures. Then, the micro-combustion occurs extremely rapidly, and the central axis temperature at $x = 0.4$ mm reaches an

extreme point of 2280 K, which is greater than the CH₄ adiabatic flame temperature (about 2130 K for $\varphi = 0.9$). The heat propagates within micro-combustors as well as along the wall, then the temperature drops to 1500 K at $x = 2.0$ mm where it stabilizes until the outlet. The temperature profile obtained is almost similar to the previous works of Norton and Vlachos [20].

The temperature evolution obtained with the Duterque model along the central axis and wall is shown in Figure 5(a). As observed, the temperature profile shows the slow ascendant evolution at the inlet, indicating a delay in the mixture ignition and the temperatures of the incoming cold reactants are maintained at 300~500 K over a distance approaching 0.28 mm. Thereafter, the temperature rises up to 950 K at $x = 0.5$ mm, where the ignition occurs. The complete combustion occurs at $x = 0.8$ mm, where the flame temperature reaches maximum of 2486 K. The position of the flame quench is at $x = 2.2$ mm, while the temperature is still at 1680 K, and the temperature value is almost kept constant until the outlet. It is clearly indicate that the temperature value in this case is seriously overestimated, although the outlet temperature in the case of simulations by Li *et al.* [33] is the same order of magnitude.

The temperature evolution obtained with the Fernández-Tarrazo model along the central axis and wall is shown in Figure 7(a). The mixture temperature at the inlet is 300 K, and it undergoes an abrupt change almost from the inlet. The maximum temperature value is reached quickly at 1606 K, barely reached, then the temperature drops drastically to about 860 K and remains almost constant until the outlet.

The temperature is generally considered as one of the most significant features to characterize the combustion process and behavior. In the context of micro-combustion, it is necessary that understanding the flame temperature for the proper selection of wall materials to micro power system [40 – 42]. The micro-combustion characteristics have been identified three major zones, i.e. pre-heating zone, combustion zone and post-combustion zone [43, 44]. In the present work, the aforementioned three zones can be observed in the case of Duterque and Mantel models.

Effect on the wall temperature

The wall temperature profiles in micro-combustors were analyzed as illustrated by Figures 3 - 7 (a) to understand the effect of one-step global chemical kinetic mechanism on the wall temperature. For each model of Mantel, Duterque and Fernández-Tarrazo, the walls are preheated to 2000 K to favor the CH₄ ignition at the beginning of the numerical simulations. The energy released by CH₄ combustion is shared between the exhaust gases and the walls as the recirculation heat once the combustion arises [45 – 47]. The outlet wall at the equilibrium is considered as reaching the temperature of the exhaust gases, while the inlet wall is cooled simultaneously by the cold mixtures at the entrance, and heated by the heat released by the CH₄ combustion. This heat recirculation is crucial to the auto-ignition of the cold mixtures at the entrance, and to the micro-flame stability.

The evolution of the wall temperature with Mantel model is shown in Figure 3(a). The steady state temperature of the wall reaches about 780 K at the inlet, evolves along the axial direction to 1480 K at the outlet. Noted that the wall and the flow zone have been initially preheated to 900 K in order to allow the micro-flame to develop. The steady state temperature of the wall is lower than that of the reaction mixtures. This behavior is

mostly because of the conjugated effects: cooling of the cold feed at the inlet; combustion arises early; sharply declining temperature along the axial direction because of the heat loss.

The evolution of the wall temperature with Duterque model is shown in Figure 5(a). The temperature of the wall reaches about 680 K at the inlet, and undergoes a considerable change at the ignition time, then reaches the maximum value of 2208 K at $x = 0.8$ mm, finally decreases slightly to 1608 K because of the heat loss. The initial temperature for both the solid wall and gas phase is 2000 K at the beginning of this simulation with Duterque model, therefore, at this high initial temperature, the micro-flame can be developed and stabilized. The flame thickness is broadened, and the temperature of the exhaust gases remains high until the outlet, which have the same temperature as the wall at the outlet. By contrast, the wall at the inlet is heated because of the high combustion temperature.

The evolution of the wall temperature with Fernández-Tarrazo model is shown in Figure 7(a). The temperature of the wall at the inlet is 1348 K and decreases slightly to 848 K because of the heat loss. The initial temperature for both the solid wall and gas phase is set at 2000 K for the aforementioned reason. Note that the initial temperatures have been amended many times for these simulations to see if the flame behavior will be different. These changes of the wall temperature have often led to a lack of the convergence and a failure of the simulation.

The wall temperature of the combustion chamber is an important parameter to improve the combustion efficiency and flame stability, because it plays the competing effect and vital role for the preheating of reactants and the stabilization of flame. The wall is critical to the flame stability and ignition in micro-channels, which has been shown in the literature [20, 30, 44, 46, 48]. The wall itself has dual and competing roles in the further heat transfer. On the one hand, it will provide a convenient path for heat transfer from the post combustion zone to preheat the cold and unburned reactants, avoiding the use of the pre-heating device. On the other hand, the wall contributes to heat exchange with the external environment; the radial heat conduction to the external environment will delay flame ignition and even cause extinction. The reported simulation results indicated that moderate wall thermal conductivity is essential for ignition and the stabilization of flame near the micro-combustor entrance [46, 48]. It is very useful for the simulations to set the initial temperature for the various chemical kinetics models, allowing the onset of ignition. In the Norton and Vlachos study [20], the initial temperature was set at 1000 K, while in that done by Li *et al.* [33], it was set at 1600 K, and for this work of three simulated models (Mantel, Duterque and Fernández-Tarrazo models with one-step global equation), it was set at 2000 K.

CONCLUSIONS

For characterizing the combustion process, the flame temperature and structure are important parameters especially in the micro-combustion, which is a master tool for the flame location and the judicious choice of wall material. Numerical investigations of the premixed methane-air flame were carried out to compare and analyze the effect of the comprehensive chemical kinetic mechanisms following Mantel, Duterque and Fernández-Tarrazo models. The micro-flame structure along with the central axis and

wall temperature were analyzed. The results appear that the one-step global chemical kinetic mechanism has a significant effect on the micro-flame shape, as seen from the flames of bamboo shoot, tulip and cone shape, using Mantel, Duterque and Fernández-Tarrazo models. The micro-flame obtained by the Duterque model presented a very hot spot and causes a broadening of the combustion zone, which increase a blowout risk with the thickness greater than 2.2 mm. The different temperatures of the flame obtained were overestimated. However, note that the burning temperature (2486 K) of the Duterque model exceeds by far the adiabatic flame temperature (about 2130 K for $\varphi = 0.9$) with a delay in the mixture ignition, because of the cold mixture accumulation at the inlet. Fernández-Tarrazo model results in a rapid extinction and doesn't seem to take all the kinetic behavior into account for the appropriate micro-combustion simulations. No particularity was observed on the wall temperature profile. Even if the one-step global chemical kinetic mechanism is associated with several simplifications, the simulation results presented show some trends, which provide a master tool and an understanding of the micro-combustion behavior.

REFERENCES

1. Miyata, E., Fukushima, N., Naka, Y., Shimura, M., Tanahashi, M., Miyauchi, T.: Direct numerical simulation of micro combustion in a narrow circular channel with a detailed kinetic mechanism, *Proceedings of the Combustion Institute*, **2015**, 35 (3), 3421-3427;
2. Wan, J., Yang, W., Fan, A., Liu, Y., Yao, H., Liu, W., Du, Y., Zhao, D.: A numerical investigation on combustion characteristics of H₂/air mixture in a micro-combustor with wall cavities, *International Journal of Hydrogen Energy*, **2014**, 39 (15), 8138-8146;
3. Wan, J., Fan, A., Liu, Y., Yao, H., Liu, W., Gou, X., Zhao, D.: Experimental investigation and numerical analysis on flame stabilization of CH₄/air mixture in a mesoscale channel with wall cavities, *Combustion and Flame*, **2015**, 162 (4), 1035-1045;
4. Jejurkar, S.Y., Mishra, D.P.: Numerical characterization of a premixed flame based annular microcombustor, *International Journal of Hydrogen Energy*, **2010**, 35 (18), 9755-9766;
5. Yuan, W., Deng, J., Zhou, B., Zhang, Z.-C., Tang, Y.: Performance of a catalytic micro-combustor based on Pt/Al₂O₃/Ni for methanol fuel cell application, *Chemical Engineering Journal*, **2014**, 251, 51-57;
6. Deng, C., Yang, W., Zhou, J., Liu, Z., Wang, Y., Cen, K.: Catalytic combustion of methane, methanol, and ethanol in mesoscale combustors with Pt/ZSM-5 packed beds, *Fuel*, **2015**, 150, 339-346;
7. Fan, Y., Suzuki, Y., Kasagi, N.: Experimental study of micro-scale premixed flame in quartz channels, *Proceedings of the Combustion Institute*, **2009**, 32 (2), 3083-3090;
8. Jackson, T.L., Buckmaster, J., Lu, Z., Kyritsis, D.C., Massa, L.: Flames in narrow circular tubes, *Proceedings of the Combustion Institute*, **2007**, 31 (1), 955-962;
9. Deshpande, A.A., Kumar, S.: On the formation of spinning flames and combustion completeness for premixed fuel-air mixtures in stepped tube microcombustors, *Applied Thermal Engineering*, **2013**, 51 (1-2), 91-101;
10. Xu, B., Ju, Y.: Experimental study of spinning combustion in a mesoscale divergent channel, *Proceedings of the Combustion Institute*, **2007**, 31 (2), 3285-3292;
11. Sirignano, W.A., Pham, T.K., Dunn-Rankin, D.: Miniature-scale liquid-fuel-film combustor, *Proceedings of the Combustion Institute*, **2002**, 29 (1), 925-931;
12. Fan, A., Maruta, K., Nakamura, H., Kumar, S., Liu, W.: Experimental investigation on flame pattern formations of DME-air mixtures in a radial microchannel, *Combustion and Flame*, **2010**, 157 (9), 1637-1642;
13. Kumar, S., Maruta, K., Minaev, S.: On the formation of multiple rotating Pelton-like flame structures in radial microchannels with lean methane-air mixtures, *Proceedings of the Combustion Institute*, **2007**, 31 (2), 3261-3268;

14. Bianco, F., Chibbaro, S., Legros, G.: Low-dimensional modeling of flame dynamics in heated microchannels, *Chemical Engineering Science*, **2015**, 122, 533-544;
15. Leu, C.-H., King, S.-C., Huang, J.-M., Chen, C.-C., Tzeng, S.-S., Lee, C.-I., Chang, W.-C., Yang, C.-C.: Visible images of the catalytic combustion of methanol in a micro-channel reactor, *Chemical Engineering Journal*, **2013**, 226, 201-208;
16. Kim, K.T., Lee, D.H., Kwon, S.: Effects of thermal and chemical surface-flame interaction on flame quenching, *Combustion and Flame*, **2006**, 146 (1-2), 19-28;
17. Yang, H., Feng, Y., Wang, X., Jiang, L., Zhao, D., Hayashi, N., Yamashita, H.: OH-PLIF investigation of wall effects on the flame quenching in a slit burner, *Proceedings of the Combustion Institute*, **2013**, 34 (2), 3379-3386;
18. Westbrook, C.K., Dryer, F.L.: Simplified reaction mechanisms for the oxidation of hydrocarbon fuels in flames, *Combustion Science and Technology*, **1981**, 27 (1-2), 31-43;
19. Kaisare, N.S., Vlachos, D.G.: Extending the region of stable homogeneous micro-combustion through forced unsteady operation, *Proceedings of the Combustion Institute*, **2007**, 31 (2), 3293-3300;
20. Norton, D.G., Vlachos, D.G.: Combustion characteristics and flame stability at the microscale: a CFD study of premixed methane/air mixtures, *Chemical Engineering Science*, **2003**, 58 (21), 4871-4882;
21. Gutkowski, A.: Numerical analysis of effect of ignition methods on flame behavior during passing through a sudden contraction near the quenching conditions, *Applied Thermal Engineering*, **2013**, 54 (1), 202-211;
22. Fernández-Tarrazo, E., Sánchez, A.L., Liñán, A., Williams, F.A.: A simple one-step chemistry model for partially premixed hydrocarbon combustion, *Combustion and Flame*, **2006**, 147 (1-2), 32-38;
23. Mantel, T., Egolfopoulos, F., Bowman, C.T.: A new methodology to determine kinetic parameters for one- and two-step chemical models in: *Proceedings of the Summer Program 1996*, Centre for Turbulence Research (CTR), Stanford University, Stanford, CA, USA, **1996**, 149-166;
24. Duterque, J., Borghi, R., Tichtinsky, H.: Study of quasi-global schemes for hydrocarbon combustion, *Combustion Science and Technology*, **1981**, 26 (1-2), 1-15;
25. Ennetta, R., Hamdi, M., Said, R.: Comparison of different chemical kinetic mechanisms of methane combustion in an internal combustion engine configuration, *Thermal Science*, **2008**, 12 (1), 43-51;
26. *Fluent 6.3 user's guide*, Lebanon, New Hampshire: Fluent Inc., **2006**;
27. Kee, R.J., Rupley, F.M., Meeks, E., Miller, J.A.: *CHEMKIN-III: A Fortran chemical kinetics package for the analysis of gas-phase chemical kinetics*, Report No. SAND96-8216, Technical Report, Sandia National Laboratories, **1996**;
28. Deshmukh, S.R., Vlachos, D.G.: A reduced mechanism for methane and one-step rate expressions for fuel-lean catalytic combustion of small alkanes on noble metals, *Combustion and Flame*, **2007**, 149 (4), 366-383;
29. Karagiannidis, S., Mantzaras, J., Jackson, G., Boulouchos, K.: Hetero-/homogeneous combustion and stability maps in methane-fueled catalytic microreactors, *Proceedings of the Combustion Institute*, **2007**, 31 (2), 3309-3317;
30. Norton, D.G., Vlachos, D.G.: A CFD study of propane/air microflame stability, *Combustion and Flame*, **2004**, 138 (1-2), 97-107;
31. Hua, J., Wu, M., Kumar, K.: Numerical simulation of the combustion of hydrogen-air mixture in micro-scaled chambers. Part I: Fundamental study, *Chemical Engineering Science*, **2005**, 60 (13), 3497-3506;
32. Li, J., Chou, S.K., Huang, G., Yang, W.M., Li, Z.W.: Study on premixed combustion in cylindrical micro combustors: Transient flame behavior and wall heat flux, *Experimental Thermal and Fluid Science*, **2009**, 33 (4), 764-773;
33. Li, J., Chou, S.K., Yang, W.M., Li, Z.W.: A numerical study on premixed micro-combustion of CH₄-air mixture: Effects of combustor size, geometry and boundary conditions on flame temperature, *Chemical Engineering Journal*, **2009**, 150 (1), 213-222;
34. Kim, N.I., Maruta, K.: A numerical study on propagation of premixed flames in small tubes, *Combustion and Flame*, **2006**, 146 (1-2), 283-301;

35. Zamashchikov, V., Tikhomolov, E.: Sub-critical stable hydrogen-air premixed laminar flames in micro gaps, *International Journal of Hydrogen Energy*, **2011**, 36 (14), 8583-8594;
36. Coltrin, M.E., Kee, R.J., Rupley, F.M.: *Surface CHEMKIN (Version 4.0): A Fortran package for analyzing heterogeneous chemical kinetics at a solid surface/gas-phase interface*, Report No. SAND90-8003B, Technical Report, Sandia National Laboratories, **1991**;
37. Manion, J.A., Huie, R.E., Levin, R.D., Burgess Jr., D.R., Orkin, V.L., Tsang, W., McGivern, W.S., Hudgens, J.W., Knyazev, V.D., Atkinson, D.B., Chai, E., Tereza, A.M., Lin, C.-Y., Allison, T.C., Mallard, W.G., Westley, F., Herron, J.T., Hampson, R.F., Frizzell, D.H.: *NIST Chemical Kinetics Database, NIST Standard Reference Database 17, Version 7.0 (Web Version)*, Release 1.6.8, Data version 2013.03, National Institute of Standards and Technology, Gaithersburg, Maryland, 20899-8320, <http://kinetics.nist.gov/>, accessed April 6, **2015**;
38. Kee, R.J., Dixon-Lewis, G., Warnatz, J., Coltrin, M.E., Miller, J.A.: *A Fortran computer code package for the evaluation of gas-phase multicomponent transport properties*, Report No. SAND86-8246, Technical Report, Sandia National Laboratories, **1986**;
39. Hackert, C.L., Ellzey, J.L., Ezekoye, O.A.: Effects of thermal boundary conditions on flame shape and quenching in ducts, *Combustion and Flame*, **1998**, 112 (1-2), 73-84;
40. Niazmand, H., Renksizbulut, M., Saeedi, E.: Developing slip-flow and heat transfer in trapezoidal microchannels, *International Journal of Heat and Mass Transfer*, **2008**, 51 (25-26), 6126-6135;
41. Renksizbulut, M., Niazmand, H., Tercan, G.: Slip-flow and heat transfer in rectangular microchannels with constant wall temperature, *International Journal of Thermal Sciences*, **2006**, 45 (9), 870-881;
42. Mlcak, J.D., Anand, N.K., Rightley, M.J.: Three-dimensional laminar flow and heat transfer in a parallel array of microchannels etched on a substrate, *International Journal of Heat and Mass Transfer*, **2008**, 51 (21-22), 5182-5191;
43. Xu, B., Ju, Y.: Concentration slip and its impact on heterogeneous combustion in a micro scale chemical reactor, *Chemical Engineering Science*, **2005**, 60 (13), 3561-3572;
44. Chen, G.-B., Chen, C.-P., Wu, C.-Y., Chao, Y.-C.: Effects of catalytic walls on hydrogen/air combustion inside a micro-tube, *Applied Catalysis A: General*, **2007**, 332 (1), 89-97;
45. Lee, D.K., Maruta, K.: Heat recirculation effects on flame propagation and flame structure in a mesoscale tube, *Combustion Theory and Modelling*, **2012**, 16 (3), 507-536;
46. Leach, T.T., Cadou, C.P., Jackson, G.S.: Effect of structural conduction and heat loss on combustion in micro-channels, *Combustion Theory and Modelling*, **2006**, 10 (1), 85-103;
47. Kessler, D.A., Short, M.: Ignition and transient dynamics of sub-limit premixed flames in microchannels, *Combustion Theory and Modelling*, **2008**, 12 (5), 809-829;
48. Choi, B.-I., Han, Y.-S., Kim, M.-B., Hwang, C.-H., Oh, C.B.: Experimental and numerical studies of mixing and flame stability in a micro-cyclone combustor, *Chemical Engineering Science*, **2009**, 64 (24), 5276-5286.